doi: 10.1255/nirn.1647

New application of hyperspectral imaging for bacterial cell classification‡

Bosoon Park

Bosoon Park* and Matthew Eady
United State Department of Agriculture, Agricultural Research Service, US National Poultry Research Center, 950 College Station Road, Athens, GA 30605, USA. E-mail: bosoon.park@ars.usda.gov

Introduction

Both *Salmonella* and *Campylobacter* are major causes of food-borne disease outbreaks in both the USA and EU. Food-borne outbreaks of *Salmonellosis* were reported to be responsible for illness in 16.4 and 22.2 cases per 100,000 people in the USA and EU, respectively. In addition, outbreaks caused by *Campylobacteriosis* were at levels of 14.3 and 55.5 cases per 100,000 people in the US and EU, respectively. For instance, more than one million people are sickened by *Salmonella* in the United States each year with approximately 200,000 cases arising from poultry sources alone,[1] resulting in an average national cost for food-borne illness of up to US$93.2 billion.[2] *Campylobacter* caused the largest number of food-borne bacterial illnesses in Denmark in 2014 at 3782 cases.

Current gold standards for *Salmonella* detection and characterisation rely on a series of pre- and selective enrichment procedures, followed by biochemical and serological confirmation all of which typically requires four to seven days. Rapid methods such as polymerase chain reaction (PCR) and enzyme-linked immunosorbent assay (ELISA) have been commercially available and applied to replace or facilitate conventional microbiological tests. Still, however, alternative techniques such as optical methods are being pursued to characterise pathogens to the serotype level in a reasonably short period of time at reduced costs.

Since hyperspectral imaging (HSI) technologies were introduced early 1980s in earth remote sensing, the technique has been applied to many other fields including medical, biological, environmental, food and agricultural areas for research and development and practical uses. In terms of food applications, different HSI platforms have been developed for quality and safety evaluation in food processing. Many researchers have demonstrated that HSI techniques have the potential to evaluate quality and safety in foods in real-time. Our research group in the US Department of Agriculture, Agricultural Research Service (USDA, ARS) in Athens, Georgia has expanded this technique through its application at a microscopic level to detect food-borne pathogenic bacteria in food matrices such as poultry carcass rinsate. This same group has developed an acousto-optic tunable filter (AOTF)-based hyperspectral microscope imaging (HMI) platform to detect food-borne pathogens at cell level.[3]

Since the significance of food-borne pathogens in public health and in food industry products calls for rapid and accurate analytical methods to be used for both detection and classification in routine inspection as well as during a food-borne outbreak, the HMI technique will be useful for food safety research and development.

Hyperspectral microscope imaging technology

Thus, hyperspectral microscope imaging (HMI) for bacterial detection and identification at the cell level is another emerging area of HSI applications. The HMI method enables us to identify bacteria with microcolony samples grown on selective agar media in about 8 h.[4] ARS researchers have developed this HMI technique to enhance the limit of detection by identifying spectral signatures of bacteria from microcolonies.

The ARS HMI system (Figure 1) consists of a Nikon upright microscope, acousto-optic tunable filters (AOTF), a high-performance cooled electron multiplying charge coupled device (EMCCD) camera and dark-field illumination lighting sources for scattering image acquisition from the single cell. For the image acquisition from live cells, immobilisation of cells and image acquisition time is crucial to obtain high-quality spectral images. The AOTF-based HMI has advantages in terms of high-speed, high-throughput, random-access optical filter with high rejected light levels and area scan ability. AOTF delivers diffraction-limited image quality with variable bandwidth resolution down to within 2 nm in the spectral range from 450 nm to 800 nm. AOTF-based HMI employs an instrumental technology with no moving parts, capable of high scan speeds and random access to any number of pre-selected wavelengths.

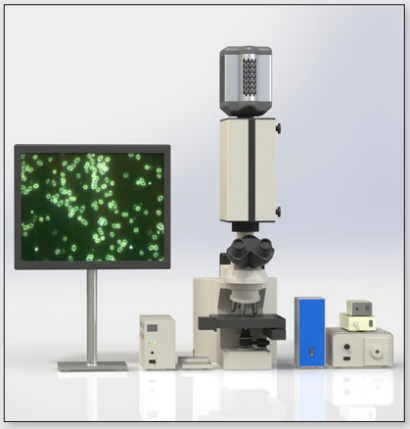

Figure 1. ARS hyperspectral microscope imaging system for bacteria detection.

With HMI techniques, food-borne pathogenic bacteria such as shiga toxin producing *E. coli* (STEC) serogroups and *Salmonella* serotypes can be identified with high detection accuracy using appropriate chemometric procedures.[5] Using this technique, gram-positive and gram-negative bacteria from chicken carcass rinsate can be classified with 99% accuracy.[6] Currently, ARS researchers are developing a database by collecting spectral signatures from many bacterial samples and food matrices to generate a spectral library "fingerprint" for each microorganism and allow the identification of unknown samples by a HMI technique.

‡Mention of trade names or commercial products in this article is solely for the purpose of providing specific information and does not imply recommendation or endorsement by the US Department of Agriculture.

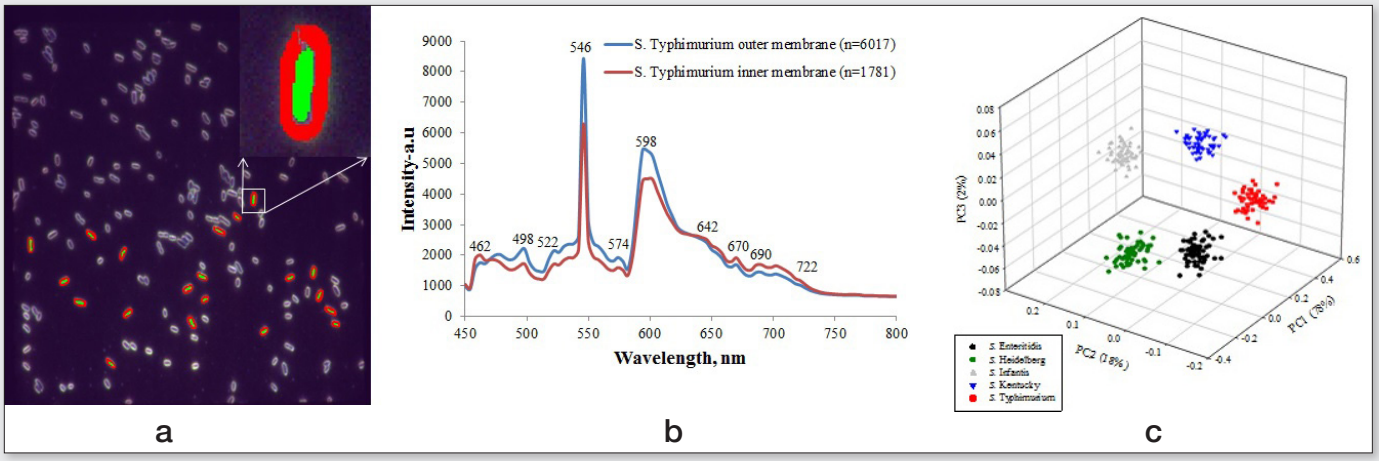

Figure 2. HMI from *Salmonella* Typhimurium (a) regions of interest (ROIs); (b) spectral signature of the cells with a metal-halide lighting source; and (c) PCA score plots for five serotypes (*S*. Enteritidis, *S*. Typhimurium, *S*, Infantis, *S*. Heidelberg, *S*. Kentucky).

HMI for *Salmonella*

ARS researchers have developed early and rapid optical methods to identify *Salmonella* serotypes by HMI.[7] Hyperspectral microscopic images from *S.* Typhimurium serotype (Figure 2) demonstrated that the spectral signatures between inner and outer cell walls (Figure 2a) were not significantly different over the spectral range between 450 nm and 800 nm although scattering intensity changed with wavelength (Figure 2b). From the results of principal component analysis, the score plot demonstrated well-separated clusters from each *Salmonella* serotype tested (Figure 2c).

Using a support vector machine (SVM) classification method, a classification accuracy of up to 99.5% using 89 selected wavelengths was obtained for *Salmonella* serotypes. As shown in Table 1, if selected wavelengths were reduced down to 20, 12 and 7 to facilitate faster and therefore more economical spectral image acquisition and processing, the classification accuracies were reduced but generally still over 90%; when only three bands were used, classification accuracy decreased to 84.3%. Thus, this HMI technique has the potential to identify *Salmonella* serotypes on the basis of their spectral signatures (scattering intensity from live cells).

HMI for *Campylobacter*

Similarly, three *Campylobacter* species including *C. coli subsp.* (Cc), *C. fetus subsp. fetus* (Cf) and *C. jejuni subsp. jejuni* (Cj) were tested using stock cultures of isolates from chicken carcass rinses. Cultures were grown on microaerophilic agar in a specialised atmospheric chamber. After incubation, sample slides were prepared for HMI acquisition.[3]

In order to obtain spectral signatures from *Campylobacter* serotypes such as *C*. coli. (Figure 3a), a single cell region of interest (ROI) (Figure 3b) extraction method was used to calculate mean spectra (Figure 3c) for individual *Campylobacter* cells. For this study, image processing was done through the use of the Environment for Visualizing Images (ENVI) software. *Campylobacter* cells are corkscrew-shaped and visually offer greater cell size and shape variance than other rod- or cocci-shaped bacteria such as *Salmonella* or *Staphylococcus*.[8] Because of this variance and difficulties associated with precision border definition of cell wall boundaries, a two-step ROI method was used. First, a spatial ROI is selected around a cell. Then minimum and maximum pixel intensity thresholds are determined at 650 nm by examination of a histogram of all pixels in the image. Individual cell ROIs are exported from ENVI into the R software program, where thresholding values are applied, removing background pixels and calculating the mean spectrum per cell.

Minimal preprocessing steps were used and consisted of normalising each cell's mean spectrum to the tungsten halogen light source, followed by applying multiplicative scatter correction (MSC). MSC was implemented to account for changes in the spectra due to physical influences such as stage positioning, hot or cold spots caused by distribution of the light source's photons, while maintaining inherent biological differences between cells.

A mean-centred principal component analysis (PCA) was then applied to visualise the interclass relationship of cells from the three species (Figure 3d). Euclidean distances (EDs) were calculated from each data point in the PC scores space to the centroid of its respective cluster to quantify cell-to-cell variance within an HMI. A principal component linear discriminant analysis (PC-LDA) was performed on the first five principal components to calculate the classification accuracy of the three species from the resulting confusion matrix.

The cumulative variance shown in Figure 3d shows that the first and second PCs explain the majority (99%) of the PCA's

Table 1. Classification accuracy for *Salmonella* serotypes.

Overall accuracy (%)	Spectral range (nm)	Number of bands	Band number reduction (%)
99.5	450–800	89	0
96.5	586–662	20	77.5
95.3	586–630	12	86.5
91.5	590–614	7	92.1
84.3	590–598	3	96.6

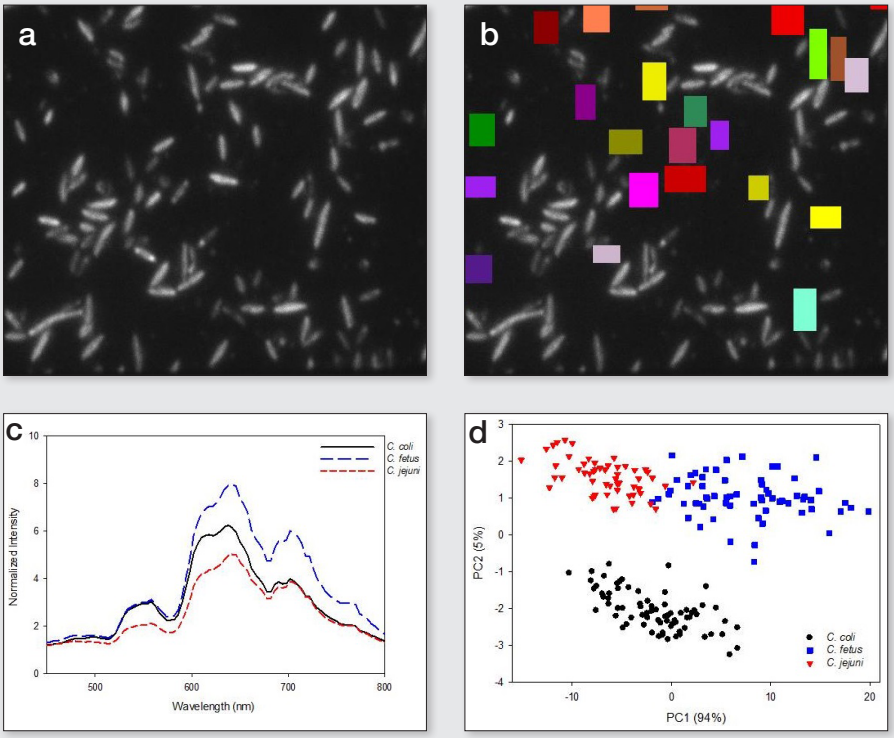

Figure 3. HMI from (a) *Campylobacter* coli; (b) regions of interest (ROI); (c) mean spectra from ROIs of *Campylobacter* species (*C.* jejuni, *C.* coli, *C.* fetus); and (d) PCA score plot.

variance. *C. coli* and *C. jejuni* are closely-related with a large number of common genes, thus presenting problems in phenotypic and biochemical differentiation between the two species.[9] From the ED values listed in Table 2, we see that *C. fetus* has the largest cell-to-cell variance. This could be attributed to differences in cell size or curvature of the corkscrew-shaped cell wall. The overall PC-LDA classification accuracy was 98.9% showing potential for HMI to differentiate between *Campylobacter* species.

In this study, image collection of HMIs required about 20 minutes. After this acquisition, ROI extraction and data analysis can be automated to take several minutes. The method shows promise as a candidate for a sensitive and rapid identification of *Campylobacter* species. Here, the trial data set shows that it is capable of discriminating between the three species but any inferences or causality should be made after future repetitions for validation.

Future HMI research

Continuing research for near infrared (NIR) HMI technology development is being conducted on the study of biochemical constituents in food-borne bacteria to better understand genotyping and serotyping using optical measurements from food-borne pathogenic bacterial cells non-destructively. Also, HMI techniques are being used to characterise nanoscale substrates for further research on food-borne bacterial detection with high sensitivity and specificity. Further HMI research will be conducted to detect multiple bacteria simultaneously with multiplex fluorescence *in situ* hybridisation (m-FISH). In addition, prototype hyperspectral sensors with selective bands will be developed for near real-time rapid detection and characterisation applications for food industry.

Table 2. Classification accuracy for *Campylobacter* subspecies.

Species	Sample size	ED $\bar{x} \pm \sigma$	PC-LDA accuracy (%)
C. coli	74	3.307 ± 2.221	100
C. fetus	64	4.504 ± 2.731	100
C. jejuni	55	2.831 ± 2.030	96.4

References

1. S. Hoffmann, B. Maculloch and M. Batz, *Economic Burden of Major Foodborne Illnesses Acquired in the United States*. USDA, ERS Report (2015). www.ers.usda.gov/publications/eib-eco-nomic-information-bulletin/eib140
2. R. Scharff, "State estimates for the annual cost of foodborne illness", *J. Food Prot*. **78,** 1064–1071 (2015). doi: https://doi.org/10.4315/0362-028X.JFP-14-505
3. B. Park, S.C. Yoon, S. Lee, J. Sundaram, W.R. Windham, A. Hinton Jr and K.C. Lawrence, "Acousto-optic tunable filter hyperspectral microscope imaging for identifying foodborne pathogens", *Trans. ASABE* **55,** 1997–2006 (2012). doi: https://doi.org/10.13031/2013.42345
4. M. Eady, B. Park and S. Choi, "Rapid and early detection of *Salmonella* serotypes with hyperspectral microscopy and multivariate data analysis", *J. Food Prot*. **78,** 668–674 (2015). doi: https://doi.org/10.4315/0362-028X.JFP-14-366
5. B. Park, W.R. Windham, S.R. Ladely, P. Gurram, H. Kwon, S.C. Yoon, K.C. Lawrence, N. Narang and W.C. Cray, "Detection of non-0157 Shiga toxin-producing *Escherichia coli* (STEC) serotypes with hyperspectral microscope imaging", *Trans ASABE* **57,** 973–986 (2014). doi: https://doi.org/10.13031/trans.57.10367
6. B. Park, Y.W. Seo, S.C. Yoon, A. Hinton, Jr, W.R. Windham and K.C. Lawrence, "Hyperspectral microscope imaging methods to classify gram-positive and gram-negative foodborne pathogenic bacteria", *Trans. ASABE* **58,** 5–16 (2015). doi: https://doi.org/10.13031/trans.58.10832
7. M. Eady and B. Park, "Classification of *Salmonella enterica* serotypes with selective bands using visible/NIR hyperspectral images", *J. Microscopy* **263,** 10–19 (2016). doi: https://doi.org/10.1111/jmi.12368
8. Y.W. Seo, B. Park, A. Hinton Jr, S.C. Yoon and K.C. Lawrence, "Identification of *Staphylococcus* species with hyperspectral microscope imaging and classification algorithms", *J. Food Meas. Char.* **10,** 253–263 (2016). doi: https://doi.org/10.1007/s11694-015-9301-0
9. I. Habib, L. De Zutter and M. Uyttendaele, "*Campylobacter* species", in *Food Microbiology: Fundamentals and Frontiers*, 4th Edn. Ed by M.P. Doyle and R.L. Buchanan. ASM Press (2013). doi: https://doi.org/10.1128/9781555818463.ch11